

## The distortion of a flexible inextensible thread in a shearing flow

By **E. J. HINCH**

Department of Applied Mathematics and Theoretical Physics,  
University of Cambridge

(Received 25 July 1975)

Using the slender-body theory for Stokes flow, the equations of motion are developed for a small flexible inextensible thread. The nearly straight thread is examined analytically, and is shown to straighten rapidly. In a simple shear flow the distortions decay less rapidly, but rapidly enough not to rotate the thread through the plane of flow. Numerical studies of simple shear with more substantially distorted threads show the same qualitative behaviour. Additionally some differences are revealed in the nonlinear regime between the buckling and stretching processes which occur in the compressive and tensile quadrants of the flow.

---

### 1. Introduction

In the study of fluid suspensions, the three basic problems in the microscopic dynamics are the rotation, deformation and interaction of the particles. Although the rotation and interaction problems are by no means easy, there has perhaps been least progress in understanding the deformation of particles in a shearing flow. Small fluid droplets with surface tension have been analysed in a near-sphere approximation; for a recent paper see Barthès-Biesel & Acrivos (1973). A viscoelastic sphere is an artificial particle which can be examined at significant distortions (Roscoe 1967). The difficulty with deformable particles is that in general an infinite number of degrees of freedom are needed to describe the distortion. This complication is serious because the problem is unavoidably non-linear (through the particle shape entering the boundary-value problem for the viscous flow of the solvent). The fluid droplets with surface tension are tractable with the near-sphere linearization, while the viscoelastic spheres require only five variables to describe their distortion by a shearing flow because their shape remains ellipsoidal. In this paper the study of a third deformable particle, a thread, is begun. The simplification available for threads is the slender-body theory for the Stokes flow of the viscous solvent surrounding the thread.

Paper pulp and asbestos fibre suspensions are two examples of industrially important suspensions of thread-like particles. In these applications the particles are probably too close together to behave like the single isolated thread to be examined in this paper. The interaction of deformable threads must be left for

the future. More dilute suspensions of threads occur in the preparation of solid composite materials containing chopped reinforcing fibres. When a dilute polymer solution is subjected to a strong flow, it is believed that the polymer molecules can be substantially stretched into a thread-like configuration. The study of threads may thus throw some light on the mechanics of highly deformed macromolecules.

For this first study of the motion of a deformable thread in a shearing flow, the thread will be made as simple as possible. By making the thread very thin, only the leading-order approximation need be retained in the slender-body theory for the Stokes flow. This leading-order approximation is notoriously inaccurate (giving 25% errors for particles with a length-to-breadth ratio of 100), but its local form for the friction forces is a crucial simplification of the dynamics of the thread. Although the poor quantitative predictions owing to the slender-body theory are unfortunate, more regrettable is the loss of some qualitative features. In simple shear a straight thread will eventually rotate across the plane of flow through the small couple from the velocity difference over the width of the thread. The approximation of slender-body theory adopted here does not include this couple. Thus in simple shear we shall find that a straight thread tends to align with the flow instead of truly rotating periodically. The internal dynamics of the thread are similarly chosen for simplicity. The thread will be inextensible but perfectly flexible. This combination means that no dimensional property of the thread is introduced: the elasticity for stretching is infinite while the stiffness for bending is zero. Although the stiffness is related to the internal elasticity, the chosen behaviour can be achieved by making the thread appropriately slender.

The basic formulation of the problem is given in the following section, and a pair of equations is derived for the evolution of the shape of the thread. The equations are linearized in §3 by making an approximation for nearly straight threads. The general solution of the linearized equations is found for axisymmetric straining and for simple shear flow. The problem in simple shear of whether small distortions can help a thread to rotate across the plane of the flow is examined in §4. Some numerical solutions of the full nonlinear equations are presented in §5. The range of validity of the linear theory is found along with some nonlinear deviations from the linear theory.

## 2. The governing equations

We consider a thin thread of length  $2L$  with a slowly varying cross-section which typically has a thickness  $2\rho$  ( $\rho \ll L$ ). The deformed shape is restricted to have curvature comparable with the length rather than the thickness. Arc length along the thread is measured by  $s$ ,  $-L \leq s \leq L$ . A suitable kinematic description of such a deforming thread is to specify the position  $\mathbf{x}(s, t)$  of the centre-line of the cross-section. Dashes and dots will be used to denote derivatives with respect to arc length and time, i.e.  $\mathbf{x}'$  and  $\dot{\mathbf{x}}$ . Thus the definition of arc length yields for every position  $s$

$$\mathbf{x}' \cdot \mathbf{x}' = 1. \quad (2.1)$$

If the thread were extensible, one might use the variable  $s$  as a Lagrangian label of material points along the thread. As the thread stretched,  $s$  could not remain the true arc-length variable, i.e. satisfying (2.1) at different times. The inextensibility of the thread is expressed by the preservation of arc length in time. Thus we have the constraint

$$\dot{\mathbf{x}}' \cdot \mathbf{x}' = 0. \quad (2.2)$$

To preserve the arc length there must be a tension  $T(s, t)$  in the thread, the Lagrangian multiplier associated with the constraint (2.2). The tension is the net force transmitted over a cross-section of the thread, and with no stiffness it must be in the direction of the unit tangent  $\mathbf{x}'$ . Because the elasticity of the thread has been assumed to be infinite, the tension is locally indeterminate. The values of the tension along the length of the thread are instead determined by the need to satisfy globally the constraint (2.2).

The tension forces in the thread must balance the viscous forces, which resist the motion of the thread relative to the ambient shearing flow. If the viscous force acting on the thread is  $\mathbf{f}(s, t)$  per unit length, then the force balance on an element of arc is

$$-\mathbf{f} = (T\mathbf{x}')' = T'\mathbf{x}'' + T'\mathbf{x}'. \quad (2.3)$$

This equation shows two orthogonal contributions from the tension. (From (2.1) note that  $\mathbf{x}'' \cdot \mathbf{x}' = 0$ .) There is a force in the direction of the unit tangent  $\mathbf{x}'$  proportional to the increase in tension along the thread  $T'$ . There is also a 'hoop' force in the direction of the normal  $\mathbf{x}''$  proportional to the tension  $T$  multiplied by the curvature  $|\mathbf{x}''|$ .

The description of the thread dynamics is completed by an expression for the fluid drag  $\mathbf{f}$ . Only the local value of the gradient of the undisturbed flow affects the changes in shape if the thread is small. Thus we consider the motion of the thread when it is placed in a time-dependent general shearing flow  $\mathbf{\Gamma}(t) \cdot \mathbf{x}$ . It is useful to split the velocity gradient  $\mathbf{\Gamma}$  into the symmetric strain rate  $\mathbf{E}$  and the antisymmetric vorticity  $\mathbf{\Omega}$ :  $\mathbf{\Gamma} = \mathbf{E} + \mathbf{\Omega}$ . From the slender-body theory ( $\rho \ll L$ ) for Stokes flow ( $\Gamma L^2/\nu \ll 1$ ), the drag  $\mathbf{f}$  per unit length is related locally in the leading approximation to the slip of the undisturbed flow relative to the moving thread,  $\mathbf{\Gamma} \cdot \mathbf{x} - \dot{\mathbf{x}}$  at each  $s$ . The friction coefficient for motion parallel to the thread is  $2\pi\mu/\ln(2L/\rho)$  and twice this for transverse motion (Cox 1970). Thus

$$\mathbf{f} = \frac{2\pi\mu}{\ln 2L/\rho} (2\mathbf{1} - \mathbf{x}'\mathbf{x}') \cdot (\mathbf{\Gamma} \cdot \mathbf{x} - \dot{\mathbf{x}}). \quad (2.4)$$

In solving the preceding system of equations it is useful to absorb the factor  $\ln(2L/\rho)/2\pi\mu$  into the tension, changing its units of measurement. First the drag force (2.4) is substituted into the force balance (2.3). To solve for the rate of distortion of the thread  $\dot{\mathbf{x}}$  the inverse  $\frac{1}{2}(\mathbf{1} + \mathbf{x}'\mathbf{x}')$  of  $2\mathbf{1} - \mathbf{x}'\mathbf{x}'$  is needed. Thus we obtain the main evolution equation for the thread, using  $\mathbf{x}' \cdot \mathbf{x}'' = 0$  from (2.1), as

$$\dot{\mathbf{x}} = \mathbf{\Gamma} \cdot \mathbf{x} + T'\mathbf{x}' + \frac{1}{2}T\mathbf{x}'' \quad (2.5)$$

The motion of the thread is the combination of three effects. It is advected by the undisturbed flow, pulled in the direction of the local tangent owing to the increasing tension along it, and pulled normal to itself by the 'hoop' tension. The coefficient of a half in (2.5) comes directly from the two-to-one ratio of the friction factors in the slender-body theory.

Supplementing the evolution equation (2.5) we need a side equation for the tension. This is clearly connected with the internal dynamics, i.e. the inextensibility constraint (2.2). From the velocity  $\dot{\mathbf{x}}$  given by (2.5), we can find the rate of change of the tangent  $\dot{\mathbf{x}}'$ . On substituting this into the constraint (2.2) and using  $\mathbf{x}''' \cdot \mathbf{x}' = -\mathbf{x}'' \cdot \mathbf{x}''$ , obtained from (2.1), we find

$$T'' - \frac{1}{2}(\mathbf{x}'')^2 T = -\mathbf{x}' \cdot \mathbf{E} \cdot \mathbf{x}'. \quad (2.6)$$

The tension is generated by the component of the strain rate  $\mathbf{E}$  in the direction of the local tangent. There is a tendency for a compression in the thread to be produced when a tensioned part is curved, the tensioned part pulling the thread towards the centre of curvature. The second-order differential equation for the tension is solved subject to the boundary conditions that the tension vanishes at the ends of the thread:

$$T = 0 \quad \text{at} \quad s = \pm L. \quad (2.7)$$

Given the shape  $\mathbf{x}(s, t)$  at one instant, the tension equation (2.6) can be solved with the boundary conditions (2.7). With the tension given at one instant, the evolution equation (2.5) gives the rate of change of shape. The initial-value problem thus requires knowledge of only the initial shape of the thread.

### 3. Nearly straight threads

The nonlinear partial differential equations (2.5)–(2.7) can be solved asymptotically when the thread is nearly straight. A straight thread in the direction of the unit vector  $\mathbf{p}(t)$ ,

$$\mathbf{x}(s, t) = \mathbf{p}(t) s,$$

rotates according to

$$\dot{\mathbf{p}} = \mathbf{\Gamma} \cdot \mathbf{p} - \mathbf{p}(\mathbf{p} \cdot \mathbf{\Gamma} \cdot \mathbf{p}). \quad (3.1)$$

As remarked in the introduction, this equation predicts in simple shear that the thread tends to align itself with the flow, when the thread really undergoes periodic rotations. However, the period of the rotations is long,  $O(L/\Gamma\rho)$ , so that there should be little difference between the true orientation and that predicted by (3.1) at any fixed finite time as the thread is made slender,  $\rho/L \rightarrow 0$ .

We now look at the behaviour of small,  $O(\epsilon)$ , deviations from a straight line, where  $\epsilon$  is a small parameter. At the lowest order, the subject of this section, we shall find the basic development of the distortions. Higher-order analyses produce small corrections to this basic development, including the important  $O(\epsilon^2)$  correction to the rotation law (3.1), which will be discussed in §4. We consider the nearly straight thread

$$\mathbf{x}(s, t) = \mathbf{p}(t)s + \epsilon \mathbf{y}(s, t), \quad (3.2)$$

with  $\mathbf{p}(t)$  satisfying (3.1). At the present order of approximation we must take  $\mathbf{p}$  orthogonal to that part of  $\mathbf{y}(s, t)$  which varies with  $s$ . More care should be exercised at higher orders, where the direction  $\mathbf{p}$  of the average straight thread must be precisely chosen and the component of the distortion parallel to  $\mathbf{p}$  subtracted out of  $\mathbf{y}(s, t)$ .

Substituting the shape (3.2) into the tension equation (2.6) gives correct to  $O(\epsilon)$

$$T'' = -\mathbf{p} \cdot \mathbf{E} \cdot \mathbf{p} - 2\epsilon \mathbf{p} \cdot \mathbf{E} \cdot \mathbf{y}'$$

with a solution satisfying the boundary conditions (2.7) given by

$$T = \mathbf{p} \cdot \mathbf{E} \cdot \mathbf{p} \frac{1}{2}(L^2 - s^2) - 2\epsilon \mathbf{p} \cdot \mathbf{E} \cdot \left( \int_{-L}^s \mathbf{y} - \frac{s+L}{2L} \int_{-L}^L \mathbf{y} \right),$$

where, as in all integrals in the paper, the integration variable is the arc length. When this expression for the tension is substituted into the evolution equation (2.5), and the rotation of the straight thread (3.1) is subtracted off, we obtain the equation for the development of  $\mathbf{y}$ :

$$\dot{\mathbf{y}} = \mathbf{\Gamma} \cdot \mathbf{y} + \mathbf{p} \cdot \mathbf{E} \cdot \mathbf{p} [-s\mathbf{y}' + \frac{1}{4}(L^2 - s^2)\mathbf{y}''] - 2\epsilon \mathbf{p} \cdot \mathbf{E} \cdot \left[ \mathbf{y} - \frac{1}{2L} \int_{-L}^L \mathbf{y} \right]. \tag{3.3}$$

From (3.3) the rate of change in time  $\dot{\mathbf{y}}$  of that part of  $\mathbf{y}$  which varies with  $s$  can be found. Using this and the rotation  $\dot{\mathbf{p}}$  from (3.1) we find

$$\partial(\mathbf{p} \cdot \mathbf{y}') / \partial t = 0 \quad \text{if} \quad \mathbf{p} \cdot \mathbf{y}' = 0.$$

Thus (3.3) implies that  $\mathbf{p}$  will remain orthogonal to that part of  $\mathbf{y}$  which varies with  $s$  if it starts off orthogonal to it. The orthogonality assumed in the definition (3.2) is therefore preserved in time.

In (3.3) there are three contributions to the change in  $\dot{\mathbf{y}}$ , only one being a change in shape. The thread drifts with a velocity  $\dot{\mathbf{a}}(t)$  which is independent of the position along the thread. With the shape remaining fixed, there is also a contribution to the change in time of the vector distortion  $\mathbf{y}$  from the rotation with the orthogonal  $\mathbf{p}(t)$ . In order to remove this rotation from the genuine distortions, the complete orthonormal triad  $\mathbf{p}$ ,  $\mathbf{q}$  and  $\mathbf{r}$  is introduced. The rotation of  $\mathbf{q}$  and  $\mathbf{r}$  arises entirely from the rotation  $\dot{\mathbf{p}}$ , i.e. we choose

$$\left. \begin{aligned} \dot{\mathbf{q}} &= -\mathbf{p}(\mathbf{q} \cdot \dot{\mathbf{p}}) = -\mathbf{p}(\mathbf{q} \cdot \mathbf{\Gamma} \cdot \mathbf{p}), \\ \dot{\mathbf{r}} &= -\mathbf{p}(\mathbf{r} \cdot \dot{\mathbf{p}}) = -\mathbf{p}(\mathbf{r} \cdot \mathbf{\Gamma} \cdot \mathbf{p}). \end{aligned} \right\} \tag{3.4}$$

The deviation  $\mathbf{y}$  from the straight thread  $\mathbf{p}s$  is now written as the sum of an accumulated drift  $\mathbf{a}(t)$  and two projections onto the rotating axes  $\mathbf{q}$  and  $\mathbf{r}$ :

$$\mathbf{y}(s, t) = \mathbf{a}(t) + \mathbf{q}(t)q(s, t) + \mathbf{r}(t)r(s, t).$$

Substituting this into (3.3) and using (3.4) yields an equation for the drift,

$$\dot{\mathbf{a}} = \mathbf{\Gamma} \cdot \mathbf{a} + \mathbf{p} \cdot \mathbf{E} \cdot \left( \frac{1}{L} \int_{-L}^L \mathbf{q}q + \mathbf{r}r \right),$$

and two equations for the genuine changes in shape,

$$\left. \begin{aligned} \dot{q} &= (\mathbf{q} \cdot \mathbf{E} \cdot \mathbf{q})q + (\mathbf{q} \cdot \mathbf{\Gamma} \cdot \mathbf{r})r + (\mathbf{p} \cdot \mathbf{E} \cdot \mathbf{p})[-sq' + \frac{1}{4}(L^2 - s^2)q''], \\ \dot{r} &= (\mathbf{r} \cdot \mathbf{\Gamma} \cdot \mathbf{q})q + (\mathbf{r} \cdot \mathbf{E} \cdot \mathbf{r})r + (\mathbf{p} \cdot \mathbf{E} \cdot \mathbf{p})[-sr' + \frac{1}{4}(L^2 - s^2)r'']. \end{aligned} \right\} \quad (3.5)$$

There remains in (3.5) a rotation without a change in shape in the vorticity part of the two coupling terms. This could be removed by modification of (3.4). Such a modification is rejected as an unnecessary complication.

The shape equations (3.5) will be solved by the method of normal modes. The eigenfunctions for the arc-length structure of the distortions are governed by

$$\frac{1}{4}(L^2 - s^2)f'' - sf' + \lambda f = 0,$$

with a regularity condition at the ends  $s = \pm L$ . This problem is solved by the first derivative of the Legendre polynomials, i.e.

$$f_n(s) = LP'_n(s/L), \quad \lambda_n = \frac{1}{4}(n^2 + n - 2) \quad \text{for } n = 1, 2, 3, \dots$$

The  $n = 1$  modes,  $f_1 = 1$ , are straight threads with nearby origins. The  $n = 2$  modes,  $f_2 = 3s/L$ , are straight threads with nearby directions. The first distortion modes are those with  $n = 3$ ,  $f_3 = 3(5s^2 - L^2)/2L^2$ , and are symmetric about the centre. Small neglected couples exerted on the thread by the shear might be expected to produce odd functions of  $s$ . The first such modes are those with  $n = 4$ :  $f_4 = 5s(7s^2 - 3L^2)/2L^3$ . These eigenfunctions are orthogonal with a quadratic weighting:

$$\langle f_n, f_m \rangle \equiv \int_{-L}^L (L^2 - s^2)f_n f_m = L^3 \delta_{nm} \frac{2n(n+1)}{2n+1}.$$

The orthogonality can be used to resolve the initial shape into the normal-mode components, and in §4 is needed to define 'the' direction of the average thread.

We now proceed to solve (3.5) by expressing the distortion in terms of the normal-mode functions:

$$\{q(s, t), r(s, t)\} = \sum_{n=1}^{\infty} \{q_n(t), r_n(t)\} f_n(s).$$

Substituting this eigenfunction expansion into (3.5) yields

$$\frac{d}{dt} \begin{pmatrix} q_n \\ r_n \end{pmatrix} = \begin{pmatrix} \mathbf{q} \cdot \mathbf{E} \cdot \mathbf{q} & \mathbf{q} \cdot \mathbf{\Gamma} \cdot \mathbf{r} \\ \mathbf{r} \cdot \mathbf{\Gamma} \cdot \mathbf{q} & \mathbf{r} \cdot \mathbf{E} \cdot \mathbf{r} \end{pmatrix} \begin{pmatrix} q_n \\ r_n \end{pmatrix} - \mathbf{p} \cdot \mathbf{E} \cdot \mathbf{p} \frac{n^2 + n - 2}{4} \begin{pmatrix} q_n \\ r_n \end{pmatrix}. \quad (3.6)$$

In a particular flow  $\mathbf{\Gamma}(t)$ , first (3.1) is solved for  $\mathbf{p}(t)$  and then (3.4) is solved for the remainder of the triad  $\{\mathbf{p}, \mathbf{q}, \mathbf{r}\}$ . Using these functions of time in (3.6), the evolution of the amplitudes  $q_n$  and  $r_n$  can be found. This solution procedure will be illustrated by two examples: axisymmetric straining flow and simple shear flow.

As a first example the 'nearly straight thread' theory is applied to a steady axisymmetric straining flow  $\mathbf{u}(\mathbf{x}, t) = E(2x, -y, -z)$ . By the symmetry about the  $x$  axis, we may place the thread in the  $x, y$  plane. Further, the origin of time may be chosen as that instant when  $\mathbf{p}$  bisects the  $x, y$  axes. Starting from these chosen initial conditions, (3.1) integrates to

$$\mathbf{p}(t) = (1, e^{-3Et}, 0)(1 + e^{-6Et})^{-\frac{1}{2}}.$$

This solution is always orthogonal to the  $z$  axis, which we now select as the constant  $\mathbf{r}(t)$ . The orthonormal triad is thus completed by

$$\mathbf{q}(t) = (-e^{-3Et}, 1, 0) (1 + e^{-6Et})^{-\frac{1}{2}}, \quad \mathbf{r}(t) = (0, 0, 1).$$

This geometrically constructed triad satisfies (3.4). With this natural triad, the amplitude equations (3.6) decouple into two first-order equations with time-dependent coefficients. The solutions are

$$q_n(t) = q_n(0) e^{-\frac{1}{2}(n^2+n)Et} \left( \frac{2}{1 + e^{-6Et}} \right)^{\frac{1}{2}(n^2+n+2)},$$

$$r_n(t) = r_n(0) e^{-\frac{1}{2}(n^2+n)Et} \left( \frac{2}{1 + e^{-6Et}} \right)^{\frac{1}{2}(n^2+n-2)}.$$

The distortions decay very rapidly, both in tensile straining ( $E > 0$ ) and compressive straining ( $E < 0$ ). In tensile straining the  $r$  and  $q$  modes eventually decay exponentially at the same rate, after an initial phase in which the  $q$  mode decreases less than the  $r$  mode by a net factor of  $\sqrt{2}$ . The first and slowest distortion modes,  $n = 3$ , have an eventual decay rate of  $6E$ , twice as high as that of the straight line approaching the  $x$  axis,  $3E$ . The first odd distortion modes,  $n = 4$ , have an eventual decay rate of  $10E$ . In compressive straining the eventual exponential decay of an  $r$  mode is less rapid than that of the corresponding  $q$  mode. Indeed, in the straight-line modes,  $n = 2$ , the  $r$  mode tends to a constant  $2^{\frac{1}{2}}r(0)$ , while the  $q$  mode has an eventual decay rate of  $3E$ . This behaviour reflects the rotation of  $\mathbf{p}(t)$ , which in general tends to the compression ( $y, z$ ) plane but has no motion in that plane. The distortion modes do not eventually decay as rapidly as in the tensile case, the decay rates being  $4.5E$  and  $1.5E$  for  $q_3$  and  $r_3$ , and  $6.5E$  and  $3.5E$  for  $q_4$  and  $r_4$ . Taking into account the fact that the strain rate  $-E$  in the direction of alignment is half the value  $2E$  of the tensile straining, the decay rates for the  $q$  modes are really larger in compressive straining, with the decay rates for the  $r$  modes an equal amount smaller.

Of practical and experimental interest is the steady simple shear flow

$$\mathbf{u}(\mathbf{x}, t) = (\gamma y, 0, 0).$$

In shear flow a straight thread sweeps out a  $\mathbf{p}(t)$  trajectory which is a great circle through the direction of flow. If we choose the time origin to be that instant when the thread passes through the orthogonal  $y, z$  plane, then (3.1) is solved by

$$\mathbf{p}(t) = (\gamma t, 1, C) [1 + C^2 + \gamma^2 t^2]^{-\frac{1}{2}},$$

with  $C$  a constant of integration. When selecting the remaining orthonormal vectors of the triad, we can conveniently take  $\mathbf{r}(t)$  to be the constant vector which defines the great circle of the above trajectory. Thus for a triad which satisfies (3.4) we have

$$\mathbf{q}(t) = (-1 - C^2, \gamma t, C\gamma t) [(1 + C^2)(1 + C^2 + \gamma^2 t^2)]^{-\frac{1}{2}},$$

$$\mathbf{r}(t) = (0, -C, 1) [1 + C^2]^{-\frac{1}{2}}.$$

Substituting this triad into the amplitude equations (3.6) and solving yields

$$r_n(t) = r_n(0) \left( \frac{1 + C^2}{1 + C^2 + \gamma^2 t^2} \right)^{\frac{1}{2}(n^2 + n - 2)},$$

$$q_n(t) = [q_n(0) + r_n(0) C \gamma t [1 + C^2]^{-\frac{1}{2}}] \left( \frac{1 + C^2}{1 + C^2 + \gamma^2 t^2} \right)^{\frac{1}{2}(n^2 + n + 2)}.$$

In shear flow the modes decay algebraically rather than exponentially. At large times the different directions of the neighbouring straight threads,  $q_2$  and  $r_2$ , decay like  $(\gamma t)^{-2}$  and  $(\gamma t)^{-1}$ . The first distortion modes  $q_3$  and  $r_3$  decay like  $(\gamma t)^{-\frac{7}{2}}$  and  $(\gamma t)^{-\frac{5}{2}}$ , while  $q_4$  and  $r_4$  decay like  $(\gamma t)^{-\frac{11}{2}}$  and  $(\gamma t)^{-\frac{9}{2}}$ . At negative times the thread is in the compressive quadrants of the shear flow, where the distortions are increasing to their maximum at  $t = 0$ . Note that the linear analysis is symmetric in time about  $t = 0$ , a property destroyed by nonlinearities.

The two preceding examples illustrate well the general behaviour of a nearly straight thread: it tends to some particular orientation and the distortions decay rapidly. Almost all flows are like tensile straining flow, with the straight thread tending to a unique direction in which it is under tension. The compressive straining flow is exceptional only in that the final direction is not unique; all the possible final alignments are under tension. In shear flow a straight thread tends to a unique direction (according to the adopted slender-body approximation), but the direction is one in which the tension vanishes. The decay of the tension as the thread aligns with the flow leads to the distortions decaying algebraically rather than exponentially.

The eventual tension in the thread is responsible for the removal of the distortions. The essential process is simply a tensioned thread snapping straight in a resistive medium. While in shear flow the tension decreases as the thread aligns with the flow, the distortions are snapped out at a faster rate than that at which the tension decreases. The details of the snapping are modified by the two-to-one ratio of the friction coefficients, coming from the slender-body theory for the Stokes flow. The effective tension in the thread is halved by the relative shielding of the parallel flows. An isotropic drag law would have decay rates of

$$\frac{1}{2}(n^2 - n) \mathbf{p} \cdot \mathbf{E} \cdot \mathbf{p},$$

associated with modal functions  $P_{n-1}(s/L)$ . At large  $n$  this is approximately twice the  $\frac{1}{4}(n^2 + n - 2) \mathbf{p} \cdot \mathbf{E} \cdot \mathbf{p}$  in the above results. (Note that the labelling has been chosen such that  $n = 3$  is the first distortion mode in both cases.) There is a secondary effect from the anisotropic friction. As the distortion decays, the thread does not move entirely in the more resisted sideways direction, but has a small velocity component along its tangent. This leads to a slight enhancement of the decay rate, by  $\frac{1}{2}(n - 2) \mathbf{p} \cdot \mathbf{E} \cdot \mathbf{p}$ , over the halved tension result

$$\frac{1}{4}(n^2 - n) \mathbf{p} \cdot \mathbf{E} \cdot \mathbf{p}.$$

In addition to the tension snapping, the basic flow itself gives an advective decrease of the thread displacement. This is the only contribution to the  $n = 2$  straight-thread modes. The magnitude of this effect depends on the direction of the distortion, thus accounting for the slight differences in behaviour between

the  $q$  and  $r$  modes. In shear flow there is no advection effect in the  $r$  mode, while the  $q$  mode benefits by an extra factor of  $[1 + C^2 + \gamma^2 t^2]^{-\frac{1}{2}}$ . It is possible for the advection effect to act negatively. On average for all directions of distortion, however, there must be advective enhancement of the decay. The vanishing of the flow divergence (i.e.  $\mathbf{\Gamma} : \mathbf{l} = 0$ ) and the stretching in the thread direction (i.e.  $\mathbf{p} \cdot \mathbf{E} \cdot \mathbf{p} > 0$ ) imply a net compression in the  $q, r$  plane.

#### 4. The crossing problem

As discussed earlier, the rotation law (3.1) for the straight thread predicts in simple shear that the thread aligns with the direction of the flow (see the solution for  $\mathbf{p}(t)$  in the worked example), whereas the thread should rotate periodically with a long period  $O(L/\rho\Gamma)$ . Missing from the slender-body approximation (3.1) is a small term  $O(\rho^2/L^2)$ . This term represents the couple which is exerted by the velocity difference across the thickness  $\rho$  of the thread. Now the nearly straight thread is in some sense given a thickness by the  $O(\epsilon)$  distortions. In this section we study whether such an effective thickness can cause the thread to cross the plane of the flow, calculating the  $O(\epsilon^2)$  correction to (3.1) which comes from the distortions. If  $\epsilon \gg \rho/L$  it is possible for the distortion correction to dominate that from the genuine thickness. The distortions also produce small,  $O(\epsilon)$ , corrections to the shape equations (3.6). These corrections are of less significance, not producing such a major qualitative change as the difference between aligning with the flow and rotating indefinitely.

For the higher-order calculation in this section, more care is needed in the kinematic description of the thread. The first problem is to define  $\mathbf{x}(s, t)$  in terms of  $\mathbf{p}(t)$  and  $\mathbf{y}(s, t)$  in such a way as to maintain  $s$  as a true arc-length variable. As before we demand that the unit vector  $\mathbf{p}(t)$  is orthogonal to that part of  $\mathbf{y}(s, t)$  which varies with  $s$ , i.e.  $\mathbf{p} \cdot \mathbf{y}' = 0$ . (The part of  $\mathbf{y}$  which is independent of  $s$  is the drift  $\mathbf{a}(t)$ , which cannot be kept orthogonal to the rotating  $\mathbf{p}(t)$ .) The arc-length condition (2.1) can be satisfied by making small adjustments to  $\mathbf{x}$  in the direction of  $\mathbf{p}$ . With a neglected error  $O(\epsilon^4)$ , we may take

$$\mathbf{x}(s, t) = \left[ s - \frac{1}{2}\epsilon^2 \int_0^s y'^2 \right] \mathbf{p}(t) + \epsilon \mathbf{y}(s, t). \quad (4.1)$$

The second problem in the kinematic description of the thread is to separate clearly the rotation from the distortions. A difficulty arises with the  $n = 2$  modes, which represent straight threads in nearby directions. A nonlinear rotation of the thread must be made to appear in  $\hat{\mathbf{p}}$  and not as a change in the amplitudes of the  $n = 2$  modes. Thus we exclude the redundant  $n = 2$  modes from  $\mathbf{y}$  at all times, defining 'the' direction of the thread to be exactly  $\mathbf{p}(t)$ . The restriction is effected using the orthogonality of the normal modes in the linear theory:

$$\langle \mathbf{y}, s \rangle \equiv \int_{-L}^L (L^2 - s^2) \mathbf{y} s = 0 \quad \text{for all } t. \quad (4.2)$$

This natural inner product is chosen because the orthogonality (4.2) of the distortions to a straight line is preserved by the linear theory.

The refined definition of the thread (4.1) is now substituted into the basic evolution equation (2.5), keeping terms  $O(\epsilon^2)$ . For  $\dot{\mathbf{p}}s$  we require that part of  $\dot{\mathbf{x}}$  which is orthogonal to  $\mathbf{p}$  ( $|\mathbf{p}| = 1$ ) and which is a linear function of arc length (straight-line mode). This part of  $\dot{\mathbf{x}}$  is extracted by employing the projection operator  $\mathbf{I} - \mathbf{p}\mathbf{p}$  in real space and  $\langle \cdot, s \rangle$  in eigenfunction space. The result of these projections, using (4.2), is

$$[\dot{\mathbf{p}} - \mathbf{\Gamma} \cdot \mathbf{p} + \mathbf{p}(\mathbf{p} \cdot \mathbf{E} \cdot \mathbf{p})] \left\langle s - \frac{1}{2}\epsilon^2 \int_0^s y'^2, s \right\rangle = \epsilon \langle T'y' + \frac{1}{2}T'y'', s \rangle.$$

A fortunate consequence of first making the two projections is that the tension need only be calculated to  $O(\epsilon)$ , i.e. to the order already obtained. Moreover the leading-order quadratic tension does not contribute because of (4.2). The corrected rotation law is finally found to be

$$\begin{aligned} \dot{\mathbf{p}} = \mathbf{\Gamma} \cdot \mathbf{p} - \mathbf{p}(\mathbf{p} \cdot \mathbf{E} \cdot \mathbf{p}) - \epsilon^2 \frac{15}{2L^5} \mathbf{p} \cdot \mathbf{E} \cdot \left[ \int_{-L}^L \left[ \left( \mathbf{y} - \frac{1}{2L} \int_{-L}^L \mathbf{y} \right) \mathbf{y}' \right. \right. \\ \left. \left. + \frac{1}{2} \left( \int_{-L}^s \mathbf{y} - \frac{s+L}{2L} \int_{-L}^L \mathbf{y} \right) \mathbf{y}'' \right] (L^2 - s^2) s \right]. \quad (4.3) \end{aligned}$$

The corrected rotation law (4.3) is applicable to all linear shearing flows. We now restrict attention to steady simple shear  $\mathbf{u} = (\gamma y, 0, 0)$ . Further, we shall investigate only the two-dimensional case in which the thread rotates and deforms in the  $x, y$  plane. Thus with  $\phi(t)$  the angle of the thread to the flow, we set

$$\mathbf{p}(t) = (\cos \phi, -\sin \phi, 0),$$

$$\mathbf{y}(s, t) = \mathbf{a}(t) + (\sin \phi, \cos \phi, 0) q(s, t).$$

The rotation law (4.3) then becomes

$$\begin{aligned} \dot{\phi} = \frac{\gamma}{2} \left\{ 1 - \cos 2\phi \left[ 1 + \epsilon^2 \frac{15}{2L^5} \int_{-L}^L \left[ \left( q - \frac{1}{2L} \int_{-L}^L q \right) q' \right. \right. \right. \\ \left. \left. \left. + \frac{1}{2} \left( \int_{-L}^s q - \frac{s+L}{2L} \int_{-L}^L q \right) q'' \right] (L^2 - s^2) s \right] \right\}. \quad (4.4) \end{aligned}$$

The thread will rotate through the plane of flow, rather than aligning with the direction of the flow, if the integral in (4.4) is negative when  $\phi = 0$ . The integral has independent contributions from the odd modes and from the even modes. On its own the first permitted mode  $n = 3$  makes the integral vanish. Thus the slowest decaying form of distortion which on its own has a non-zero integral is the  $n = 4$  mode, and this gives a negative integral  $-\frac{10}{3}q_4^2 L^3$ . The integral can be positive for some combinations of modes, e.g.  $f_5 - 2f_3$ .

In the higher-order analysis of (4.4) the thread can pass through the direction of the flow,  $\phi = 0$ , if it has a suitable distortion such as the  $n = 4$  mode when it is in the flow direction. We now consider the approach of the thread to the flow

direction with a small distortion consisting of just the  $n = 4$  mode. At small angles to the flow plane the governing equations become

$$\begin{aligned}\gamma^{-1}\dot{\phi} &= \phi^2 + \frac{2.5}{2}\epsilon^2 q_4^2 L^{-2}, \\ \gamma^{-1}\dot{q}_4 &= \frac{1.1}{2}\phi q_4 + O(\epsilon q_4^2 L^{-1}).\end{aligned}$$

If these equations are started with moderate values of  $\phi$  ( $< 0$ ) and  $q_4$ , we find for  $t < 0$

$$\begin{aligned}\phi &\sim (-\gamma t)^{-1} + \frac{2.5}{1.6}\epsilon^2 q_4^2(0) L^{-2} (-\gamma t)^{-10}, \\ q_4 &\sim q_4(0) (-\gamma t)^{-1.1} + O(\epsilon q_4^2(0) L^{-1} (-\gamma t)^{-10}).\end{aligned}$$

The potentially useful distortion decays away much faster than the thread rotates. Thus the distortion vanishes before the thread reaches the flow direction, and so the thread does not manage to rotate through the flow direction. While far beyond the range of their validity, the equations for  $\phi$  and  $\epsilon q_4$  suggest the thread will not cross the flow direction unless at the initial instant

$$5\epsilon q_4 > -3\phi L,$$

corresponding to a necessary maximum displacement  $\epsilon q(s, t)$  of  $6L$  at  $\phi = -1$ . We may thus speculate that a thread which does rotate through the flow direction must pass through an orientation at which it is substantially different from straight, where the concepts of its direction and of its rotation through the direction of flow are unclear. [This speculation is based on an analysis which neglects the velocity difference across the thread.]

The above analysis has shown that the slowest decaying mode which is potentially useful decays too rapidly for a crossing of the flow direction. We may therefore conclude that an arbitrarily distorted, nearly straight thread, the only case for which the crossing problem is meaningful, will not cross. Essentially the distortions are higher eigenmodes than the straight-thread modes  $n = 2$ . These higher modes have higher decay rates than the straight modes. Thus the strength which they have to cause a crossing decreases rapidly from the initial instant.

## 5. A numerical study

The full nonlinear equations (2.5)–(2.7) have been studied numerically in the case of a steady simple shear flow with the thread in the plane perpendicular to the vorticity vector. The thread was split into a finite number of elements of equal size  $\Delta s$ . For some of the nonlinear phenomena unequal arc lengths might have economically improved the accuracy. A spatially second-order form of the evolution equation was found by considering the force balance on a numerical element, rather than simply finite differencing the differential equation (2.5). The side equation for the tension was developed similarly from the underlying physics, choosing the tension in each element such that its arc length was preserved numerically. By thus deriving a numerical version of (2.5)–(2.7), a spatially second-order scheme was devised which avoided the unnecessary introduction at each time step of an error  $O(\Delta s^2)$  in the length of the thread. The

tension equation was in the form of a triadiagonal matrix which was to be solved by the fast double-pass technique.

The time-stepping was made by an explicit second-order scheme. The temporally second-order accuracy is more accurate than is justified by the spatial accuracy. The additional accuracy was, however, found useful, particularly for the rotation of a straight thread. The explicit time-stepping did introduce a small error  $O(\Delta s^2 \Delta t)$  in the length of the thread, as all explicit schemes must. Attempts to construct an implicit length-preserving scheme proved fruitless because of the severe nonlinearity of the constraint (2.1). A length-correcting routine was therefore applied after each time step. Points along the thread were repositioned such that the length between them was rescaled to  $\Delta s$  while maintaining the direction of each element. In this process it was found useful to stop drift of the thread by keeping its centre fixed, thus making easier the comparison of the shapes at different times.

A first check of the program was that a straight thread remained undeformed. The rotation of the straight thread provided a test of the time-stepping scheme. Second-order,  $O(\Delta t^2)$ , behaviour was noted, giving an accuracy of  $\frac{1}{2}\%$  with  $\gamma \Delta t = \frac{1}{2}$ . Numerical stability tests were performed using a small cubic seed distortion. The stability boundary was found to be  $\gamma \Delta t \lesssim 4\Delta s^2/L^2$  corresponding to  $\Delta x < \frac{1}{2}\Delta s$  with a tension of  $\frac{1}{4}\gamma L^2$ .

The first distortion problem studied with the numerical model was the decay of the  $n = 4$  mode. At low  $\epsilon q_4$  amplitudes this provides a check on the program and the linear analysis, as well as a verification of the second-order spatial accuracy of the scheme. From the worked example in §3 we have theoretically

$$q_4(t) = q_4(0) (1 + \gamma^2 t^2)^{-\frac{1}{2}} = q_4(0) |\sin \phi|^{\frac{1}{2}}.$$

A difficulty with the investigation was the difference between the theoretical  $n = 4$  mode used for the initial conditions and the numerical  $n = 4$  mode at a finite  $\Delta s$ . Inevitably the initial shape is contaminated by a contribution from the  $n = 2$  straight-line mode, which decays more slowly and eventually swamps the distortion. This troublesome lower mode was filtered out by measuring the distortion relative to the tangent at the centre, this incidentally being taken to define  $\phi$ . For the test of the linear analysis an initial amplitude of  $\epsilon q_4 = \frac{1}{75}\Delta s$  was used, producing a small end deflexion of  $0.23\Delta s$ . The initial orientation was perpendicular to the flow,  $\phi = -\frac{1}{2}\pi$ . The results for three different  $\Delta s/L$  using  $\gamma \Delta t = 0.05$  are shown in figure 1, in which the scaled distortion

$$\epsilon q(s, t)/\Delta s |\sin \phi(t)|^{\frac{1}{2}}$$

is plotted against  $s$ . The scaled distortion should remain constant in time. By  $\gamma t = 5$  the thread is  $0.2$  rad from the direction of the flow with the distortions having decayed by a factor of  $1.3 \times 10^{-4}$ . These numerical values illustrate extreme rapidity of the decay of the distortions. Within the context of a ten-thousand fold decrease in the unscaled distortions, the numerical results in figure 1 for the scaled distortions are very reasonably constant. The eigenmode structure and the decay rate are confirmed. The behaviour of the errors is consistent with second-order spatial accuracy. With the finest resolution  $\Delta s/L = \frac{2}{17}$ ,

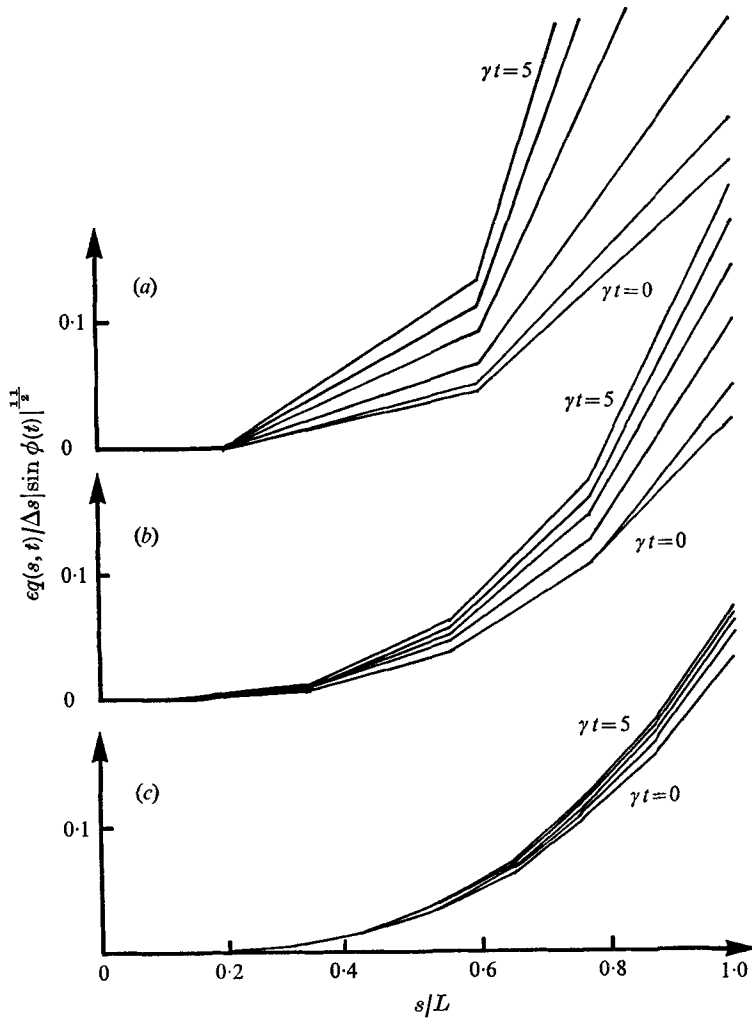


FIGURE 1. Confirmation of the linear analysis. The scaled distortion  $eq(s, t)/\Delta s |\sin^2 \phi(t)|^{1/2}$  is plotted against  $s/L$  at  $\gamma t = 0, 1, 2, 3, 4, 5$ . (a)  $\Delta s/L = \frac{2}{5}$ . (b)  $\Delta s/L = \frac{2}{3}$ . (c)  $\Delta s/L = \frac{2}{7}$ .

there is a 4% error in the scaled distortion and an error of less than 1% in the unscaled distortion during each unit time interval  $1/\gamma$ .

After confirming the eigenmode  $P'_4$  with its decay rate in the linear regime, the program was run with larger amplitudes in order to establish the range of validity of the linear theory. The initial amplitudes used were  $eq_4(0)/L = 0.094, 0.18, \pm 0.37, 0.75$  and  $\pm 1.5$ . After the initialization of  $\epsilon y(s, t)$  these large amplitudes required an immediate application of the length-correction routine to  $\mathbf{x}(s, t)$ , so that the numerical elements all started with the same arc length  $\Delta s$ . The deflexions of the end of the thread corresponding to the initial amplitudes following the length-correction procedure were  $0.27L, 0.42L, \pm 0.58L, 0.65L$  and  $\pm 0.53L$ . The largeness of the distortions is exhibited by the fact that these end deflexions do not increase by a factor of two. As before, the distortion  $eq(s, t)$

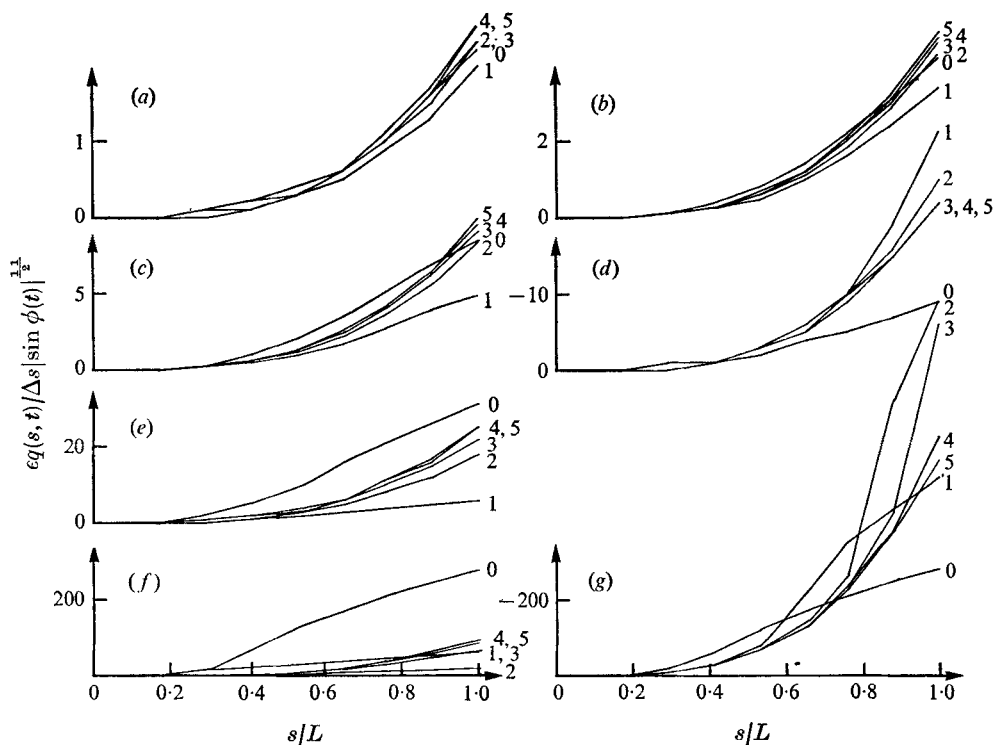


FIGURE 2. The range of validity of the linear analysis. The scaled distortion  $eq(s, t)/\Delta s |\sin \phi(t)|^{\frac{1}{2}}$  is plotted against  $s/L$  at  $\gamma t = 0, 1, 2, 3, 4, 5$ . Initial amplitudes are (a)  $eq_4(0)/L = 0.094$ , (b)  $0.18$ , (c)  $0.37$ , (d),  $-0.37$ , (e)  $0.75$ , (f)  $1.5$  and (g)  $-1.5$ .

was measured relative to the central tangent, which also was taken to define  $\phi(t)$ . While perhaps distorting some of the results, these arbitrary definitions are self-evident in the nonlinear regime, where the concepts of the distortion and orientation of a straight thread become unclear. In all the runs presented  $\gamma t = 0.05$  and  $\Delta s/L = \frac{2}{17}$ . Spot checks confirmed that these values gave a general accuracy of 1 %.

The numerical results of this second study are shown in figure 2. The scaled distortion  $eq(s, t)/\Delta s |\sin \phi(t)|^{\frac{1}{2}}$  is plotted against  $s$ . With an initial amplitude  $eq_4(0) = 0.094L$ , the shape remains within 15 % of that predicted by the linear theory. (The linear theory predicts that the scaled distortion remains constant in time.) Some of the error at larger times may be numerical. The agreement is good considering that the initial end displacement is 25 % of the half-length of the thread. The linear theory continues to agree to within a factor of two up to an initial amplitude  $eq_4(0) = 0.37L$ . At this amplitude the end displacement has risen to 60 % of the half-length of the thread. In the cases of nonlinear initial amplitudes, the linear theory becomes applicable once the distortions have decayed sufficiently. Figure 2 shows the scaled distortion settling down to the eigenfunction with a constant amplitude, this eventual amplitude no longer being the same as the initial scaled amplitude.

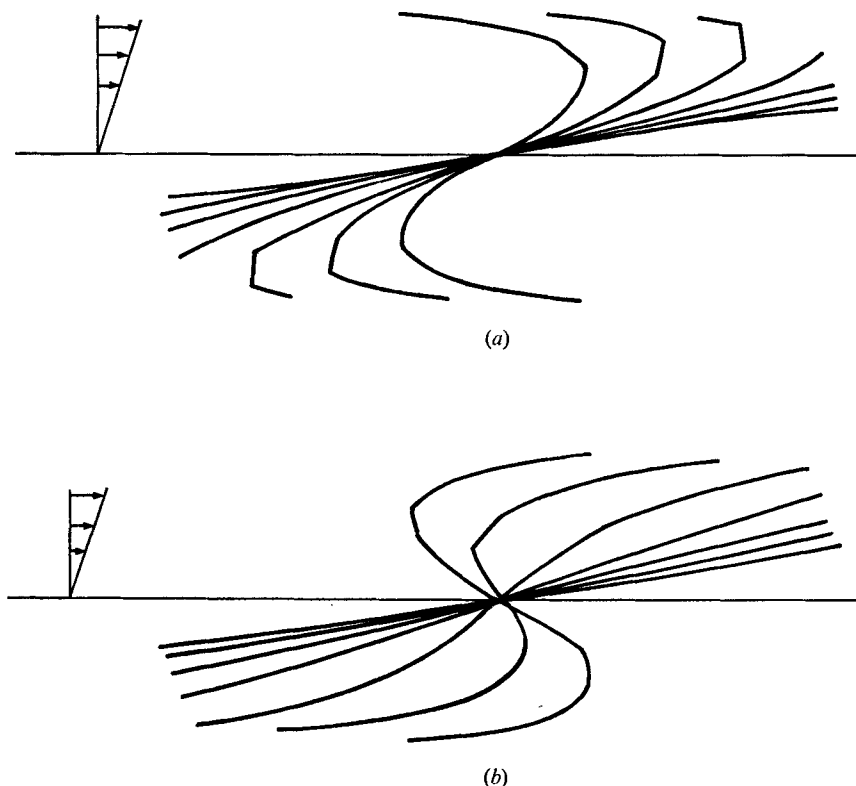


FIGURE 3. The different motions for positive and negative distortions. The configuration  $\mathbf{x}(s, t)$  is plotted against  $s$  at  $\gamma t = 0, 1, 2, 3, 4, 5, 6$ . Initial amplitudes are (a)  $\epsilon q_4 = -1.5L$  and (b)  $\epsilon q_4(0) = +1.5L$ .

Some of the nonlinear effects shown in figure 2 are probably due to the method of presenting the data. The arbitrary definition of  $\phi$  leads at small times to a suppression of positive amplitudes and an enhancement of negative amplitudes. Once the thread has straightened sufficiently this temporary effect vanishes, and a genuine nonlinear effect is revealed. There is a difference between positive and negative distortions. Figure 2 shows that the eventual amplitude of the scaled distortion attained in the quasi-linear regime is below the initial amplitude for positive distortions but above that for negative distortions. The reduction is by a factor of 3 for  $\epsilon q_4(0) = 1.5L$ , compared with an amplification of two for  $\epsilon q_4(0) = -1.5L$ . The mechanics behind this nonlinear effect are suggested in figure 3, in which the full configuration of the thread  $\mathbf{x}(s, t)$  is shown. The free end of the thread appears to be advected just in  $0 \leq \gamma t \leq 2$ . Such pure advection reduces the curvature near the end for positive distortion, but enhances it for negative distortion. The enhanced curvature corresponds to an increase in the amplitude of the linearized mode. The difference in behaviour between positive and negative distortions is equivalent to the buckling in the compressive quadrant when  $t < 0$  differing from the stretching in the tensile quadrant when  $t > 0$ . Thus the nonlinearities destroy the symmetry in time possessed by the linear modes.

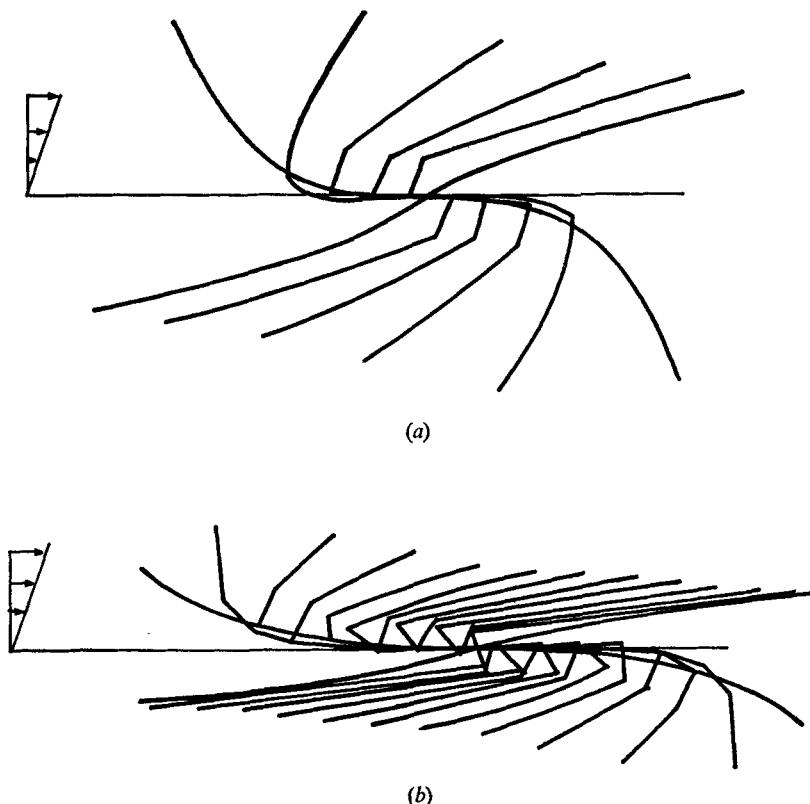


FIGURE 4. Two parts of the nonlinear phase: the rotation of the end and the advection of the outer straight sections. The configuration  $\mathbf{x}(s, t)$  is plotted against  $s$  at intervals of time  $1/\gamma$ . The initial shapes are cubics in the compressional quadrants with the central tangent in the flow direction.

The analysis in §4 for the crossing problem is confirmed by the cases studied. As seen in figure 3, the distortion is dramatically removed before the thread aligns with the flow. The distortions cannot therefore cause a crossing. The largest distortion ( $\epsilon q_4(0) = \pm 1.5L$ ) decays so much that it is barely detectable by eye at the time  $\gamma t = 4$ , when the thread is still  $14^\circ$  from the flow direction. The nonlinear phenomenon of the lack of time symmetry is also relevant to the crossing problem. A thread which managed to cross once with a positive distortion may not cross again. The nonlinearities reduce the eventual amplitude in the quasi-linear phase at the end of the tensile quadrant, when  $\gamma t \gg 1$ , compared with that at the beginning of the compression phase, when  $-\gamma t \gg 1$ . The amplitude  $\epsilon q_4(0) = 1.5L$  is attenuated by a factor of six. Of course the opposite remarks apply to negative distortions. Experiments in shear flow by Forgacs & Mason (1959) showed that a thread did cross the flow direction with a shape like the positive distortion. At this stage we must therefore suspect that the observed motion is due to effects neglected in the primitive model of this paper.

Two final numerical experiments were made in the fully nonlinear regime. The initial shapes chosen were cubics in the compressive quadrant with the

central tangent parallel to the flow. As shown in figure 4, the thread soon entered a nonlinear phase which was poorly treated by the numerical resolution available. This figure suggests that this nonlinear phase might be split into two distinct parts. First the ends turn over rapidly. That portion of the thread which starts approximately parallel to the end appears roughly to rotate like a freely hinged straight segment until an S-shape is formed. In the second part of the nonlinear motion, the outer straight sections appear to slip past the central segment virtually through pure advection, growing as they peel off the thread from the central segment. The numerical calculations indicate that large curvature occurs at the peel-off point, although this is not treated accurately. Further study of this nonlinear behaviour is required. At the end of the nonlinear phase the thread straightens, still some way before aligning with the flow. During the nonlinear phase there is substantial attenuation between the initial and final effective linear amplitudes, which makes a crossing impossible.

## REFERENCES

- BARTHÈS-BIESEL, D. & ACRIVOS, A. 1973 *J. Fluid Mech.* **61**, 1.  
COX, R. G. 1970 *J. Fluid Mech.* **44**, 791.  
FORGACS, O. L. & MASON, S. G. 1959 *J. Colloid Sci.* **14**, 473.  
ROSCOE, R. 1967 *J. Fluid Mech.* **28**, 273.